Theory of the anharmonic linewidths of surface phonons in aluminum

A. Franchini and G. Santoro
Dipartimento di Fisica, Università degli Studi di Modena, Via Campi 213/A, 41100 Modena, Italy

V. Bortolani,* A. A. Maradudin, and R. F. Wallis
Department of Physics, University of California, Irvine, California 92717
and Institute for Surface and Interface Science, University of California, Irvine, California 92717
(Received 12 November 1991)

A theoretical investigation has been made of the linewidth of the Rayleigh mode on the Al(111) surface due to cubic anharmonic interactions between atoms. The normal-mode frequencies and eigenvectors for the harmonic crystal were calculated by using a model containing central interactions extending up to tenth-nearest neighbors and three-body interactions extending up to second-nearest neighbors. This model reproduces with great accuracy the experimental bulk-phonon frequencies as well as the surface-phonon frequencies. The linewidths were evaluated along the $\bar{\Sigma}$ direction as a function of the lateral momentum transfer and at the $\bar{M}$ point as a function of the temperature. The results compare favorably with recent experimental data.

I. INTRODUCTION

The study of anharmonicity is of fundamental importance in understanding the thermal and elastic properties of solids. An important manifestation of anharmonicity appears in the one-phonon cross section,[1-3] which can be studied experimentally with scattering techniques. Anharmonic interactions produce a broadening and an energy shift of the observed peaks with increasing temperature. Neutron inelastic scattering experiments have been performed to obtain the linewidth and energy shift for bulk phonons in metals.[4,5]

Recently, there has been increasing interest in this problem in connection with the study of crystal surfaces. Theoretical as well as experimental studies have demonstrated the importance of the surface. For instance, it has been shown for certain surfaces that melting begins in the surface region.[6-8] The surface-initiated melting for Pb(100) was related to the increase with temperature of surface anharmonicity effects. The molecular-dynamical calculations for low-index Cu surfaces reported by Jayanthi, Tosatti, and Pietronero[9] indicated a larger increase with temperature of the mean-square displacement of surface atoms than of bulk atoms. Recently, Armand and Zeppenfeld[10] reported measurements of the thermal attenuation of the specular beam in He-atom surface scattering and interpreted their results in terms of an enhanced surface anharmonicity.

In the present paper we report the results of theoretical studies of the linewidths of surface phonons on aluminum that have been recently measured with high-resolution inelastic He-atom surface scattering as a function of the lateral momentum for the (111) face.[11] We use one-phonon scattering theory,[3] including cubic anharmonic terms in the crystal Hamiltonian, to investigate to what extent the linewidth evaluated in this approximation compares with the experimental data. To this end we first evaluate the linewidth as a function of the phonon momentum for the (111) surface at constant temperature. Temperature effects for some selected phonons in the surface Brillouin zone (SBZ) are also studied.

We use the lattice dynamical approach that we have recently applied to the study of bulk anharmonicity in fcc metals.[12] The harmonic model that we use is based on central and three-body interactions and satisfies rotational invariance at the surface. As shown elsewhere, this model reproduces the measured bulk[13] and surface[14] phonon frequencies. The cubic anharmonic part contains central interactions up to third-nearest neighbors. We evaluate the width of the surface phonons by performing the sums over wave vectors with 1,000 points in the SBZ. The results are compared with the recent experimental data of Toennies *et al.*[11]

II. LATTICE DYNAMICAL MODEL

The model that we use consists of a harmonic part which contains long-range central interactions, up to tenth-neighbor shells, with both the first and second derivatives of the potential for each neighbor, and angular interactions involving triplets of first- and second-nearest neighbors. The force constants of this model compare very well with the *ab initio* pseudopotential calculations performed both for the bulk and the surface.[13] The central interactions needed to correctly reproduce the Friedel oscillations present in the pseudopotential calculation include ten shells of neighbors. The numerical values of the force constants are given in Ref. 13. The force constants are defined as follows. The first-order tangential force constants α_i are

$$\alpha_i = \frac{1}{r}\frac{\partial \phi}{\partial r}\bigg|_{r=r_i}, \tag{1}$$

where r_i is the equilibrium distance of the ith atom from

the reference atom and ϕ is the central two-body potential. The second-order radial force constants β_i are

$$\beta_i = \left. \frac{\partial^2 \phi}{\partial r^2} \right|_{r=r_i} . \tag{2}$$

The three-body noncentral angular interactions are represented by a second-order nearest-neighbor angular force constant δ_l defined by

$$\delta_l = \frac{1}{3a^2} \left. \frac{\partial^2 \phi_{\theta_l}(\cos\theta_{ijk})}{\partial(\cos\theta_{ijk})^2} \right|_{\theta_{ijk}=\theta^0_{ijk}} , \quad l=1,2 \tag{3}$$

where ϕ_{θ_l} is the angular part of the potential, a is the edge of the unit cube, θ^0_{ijk} is the angle formed by the vectors $\mathbf{R}(i)-\mathbf{R}(j)$ and $\mathbf{R}(i)-\mathbf{R}(k)$, and $\mathbf{R}(i)$ is the equilibrium position vector of the ith atom. θ_1 involves a triplet of nearest-neighbor atoms, while θ_2 involves a nearest-neighbor and a second-nearest-neighbor atom.

The cubic anharmonic potential contains central interactions that extend up to third neighbors. The third-order central force constants are defined as

$$\gamma_i = r \left. \frac{\partial^3 \phi}{\partial r^3} \right|_{r=r_i} . \tag{4}$$

The cubic force constants are determined by a proper fit of the third-order elastic moduli by using the procedure developed in Ref. 12. As shown there for Al, three-body anharmonic interactions can be neglected. The third-order central force constants which best fit the experimental third-order elastic moduli extend up to the third shell of neighbors. The introduction of the second- and third-neighbor interactions is important in order to obtain numerical convergence in the values of the nearest-neighbor force constant γ_1 which is the most important ingredient in the evaluation of the linewidth.[12] The numerical values of the γ_i that we have obtained by using the harmonic model that includes ten shells of neighbors for the central interactions and two shells of neighbors for the angular forces ($10C2A$) as well as the experimental third-order elastic moduli[15] are reported in Table I.

The surface lattice dynamical problem is solved by using the slab method. In order to perform the very intensive calculations of the linewidth, which involve many diagonalizations of the dynamical matrix, we have chosen a slab with the smallest number of layers that is sufficient to avoid interference effects between the surface modes localized on opposite surfaces of the slab. We found that a slab of $N_Z=15$ atomic planes fulfills this requirement for all the lateral momenta $\mathbf{Q}$ (three-dimensional momentum projected on the surface) with $Q \geq 0.2$ Å^{-1}. In the small-Q region one should take a very large number of planes, but in this case the evaluation of the linewidth would become overwhelmingly time consuming.

We want to point out that, for the simple metal Al, there is only a small modification of the force constants in the surface region compared to the bulk region for the (111) and (100) surfaces, as demonstrated by the pseudopotential calculations of the force constants performed by Gaspar *et al.*[16] For this reason we perform our calculations by taking the same force constants in the surface region as in the bulk region.

TABLE I. The C's are the third-order elastic moduli from Ref. 15. The γ_i are the cubic-central-force constants derived with the fitting procedure of Ref. 12. The units are 10^{12} dyn/cm^2.

$C_{111}=-12.24$
$C_{112}=-3.73$
$C_{123}=0.25$
$\gamma_1=-6.33$
$\gamma_2=-1.33$
$\gamma_3=0.14$

We solve the dynamical problem for the slab of $N_Z=15$ atomic planes with one atom per unit surface cell of area A at fixed lateral momentum $\mathbf{Q}$. The eigenvalues and eigenvectors are written, respectively, as $\omega(\mathbf{Q},J)$ and $\mathbf{e}(\mathbf{Q},J;l)$. The vector $\mathbf{e}$ refers to three-dimensional Cartesian axes, l labels the planes, and J is the normal coordinate index, with $J=1,2,\ldots,3N_z$. The polarization vectors are normalized as

$$\sum_l |\mathbf{e}(\mathbf{Q},J;l)|^2 = 1 . \tag{5}$$

For surface modes, $|\tilde{e}(\mathbf{Q},J;1)|^2 \approx 1$, and for bulk modes,

$$|\mathbf{e}(\mathbf{Q},J;l)|^2 \propto \frac{1}{N_Z} . \tag{6}$$

III. FOURIER-TRANSFORMED ANHARMONIC COEFFICIENTS

The principal quantity that enters into the evaluation of the one-phonon line width Γ is the Fourier-transformed anharmonic coefficient. To determine it, we will consider the contribution of cubic anharmonic terms to the total energy of the crystal. In the case of Al, as already discussed, we consider only central cubic interactions extending up to and including the third shell of neighbors.

If we restrict ourselves to central forces, the cubic anharmonic potential for the surface problem can be written as

$$\phi_3 = \tfrac{1}{12} \sum_i \sum_{L,l} \sum_{L',l'} \sum_{\alpha,\beta,\gamma} \phi^{(i)}_{\alpha\beta\gamma}(L-L';l,l') u_\alpha(L,l;L',l') \times u_\beta(L,l;L',l') u_\gamma(L,l;L',l') , \tag{7}$$

where i specifies the interaction between ith neighbors, (L,l) designates the atom in the Lth two-dimensional unit cell of the lth atomic layer parallel to the surface,

$$\phi^{i}_{\alpha\beta\gamma}(L-L';l,l')=\left[\frac{r_\alpha r_\beta r_\gamma}{r^4}(\gamma_i-3\beta_i+3\alpha_i)+\frac{r_\alpha\delta_{\gamma\beta}+r_\beta\delta_{\gamma\alpha}+r_\gamma\delta_{\alpha\beta}}{r^2}(\beta_i-\alpha_i)\right]_{\mathbf{r}=\mathbf{R}(L-L';l,l')}, \tag{8}$$

$$\mathbf{R}(L-L';l,l')=\mathbf{R}(L,l)-\mathbf{R}(L',l') , \tag{9}$$

and

$$u_\alpha(L,l;L',l')=u_\alpha(L,l)-u_\alpha(L',l') . \tag{10}$$

The vector $\mathbf{u}(L,l)$ is the displacement of atom (L,l) from its equilibrium position. It should be emphasized that the indices (L,l) and (L',l') of a given term must be consistent with the index i. To properly include the lack of symmetry in the direction normal to the surface that we will call z, the atomic position vector is conveniently written as

$$\mathbf{R}(L,l)=\mathbf{R}(L)+\mathbf{R}(l) , \tag{11}$$

where $\mathbf{R}(L)$ specifies the origin of the Lth unit cell in the two-dimensional periodic lattice parallel to the surface and $\mathbf{R}(l)$ is the basis vector that specifies both the z coordinate of an atom and the origin of the two-dimensional lattice in the lth plane.

To describe the (111) surface, we consider a slab of (111) planes. The stacking of the planes with hexagonal symmetry is of the type $ABC\ ABC\cdots$. We consider a slab formed with an odd number of (ABC) triplets and we take the origin in the central plane. We then have

$$\mathbf{R}(L)=L_1\mathbf{a}+L_2\mathbf{b} , \tag{12}$$

with

$$\mathbf{a}=a_0\hat{\mathbf{x}} , \tag{13a}$$

$$\mathbf{b}=a_0\left[\tfrac{1}{2}\hat{\mathbf{x}}+\frac{\sqrt{3}}{2}\hat{\mathbf{y}}\right] , \tag{13b}$$

and L_1,L_2 integers.

For the basis we have

$$\mathbf{R}(l)=l\left[\tau+\frac{a_0}{2}\hat{\mathbf{x}}+\frac{\sqrt{3}}{6}\hat{\mathbf{y}}\right],\quad l=0,\pm1,\ldots,\pm l_z \tag{14}$$

with

$$\tau=\frac{2}{\sqrt{2}}\frac{a_0}{3}\hat{\mathbf{z}} , \tag{15}$$

$l_z=\frac{1}{2}(N_g-1)$, and a_0 the nearest-neighbor distance.

The Fourier-transformed coefficients of the cubic anharmonic potential are determined by using the normal coordinate representation

$$u_\alpha(L,l)=\sum_{\mathbf{Q},J}[\hbar/2NM\omega(\mathbf{Q},J)]^{1/2}e_\alpha(\mathbf{Q},J;l)\times e^{i\mathbf{Q}\cdot\mathbf{R}(L)}A_{\mathbf{Q}J} , \tag{16}$$

where $A_{\mathbf{Q}J}$ is the normal coordinate and N is the number of unit cells in the plane. To simplify somewhat the notation, we put $\mathbf{R}(L)=\mathbf{L}$. Substituting Eq. (16) into Eq. (8), we get

$$\phi_3=\sum_{\mathbf{Q},J}\sum_{\mathbf{Q}',J'}\sum_{\mathbf{Q}'',J''}V(\mathbf{Q},J;\mathbf{Q}',J';\mathbf{Q}'',J'')\times A_{\mathbf{Q}J}A_{\mathbf{Q}'J'}A_{\mathbf{Q}''J''} , \tag{17}$$

where

$$\begin{aligned}V(\mathbf{Q},J;\mathbf{Q}'J';\mathbf{Q}'',J'')&=\tfrac{1}{12}(\hbar/2NM)^{3/2}[\omega(\mathbf{Q},J)\omega(\mathbf{Q}',J')\omega(\mathbf{Q}'',J'')]^{-1/2}\\&\times\sum_i\sum_{L,l}{\sum_{L',l'}}'\sum_{\alpha,\beta,\gamma}\phi^{(i)}_{\alpha\beta\gamma}(L-L';l,l')[e_\alpha(\mathbf{Q},J;l)e^{i\mathbf{Q}\cdot\mathbf{L}}-e_\alpha(\mathbf{Q},J;l')e^{i\mathbf{Q}\cdot\mathbf{L}'}]\\&\times[e_\beta(\mathbf{Q}',J';l)e^{i\mathbf{Q}'\cdot\mathbf{L}}-e_\beta(\mathbf{Q}',J';l')e^{i\mathbf{Q}'\cdot\mathbf{L}'}][e_\gamma(\mathbf{Q}'',J'';l)e^{i\mathbf{Q}''\cdot\mathbf{L}}-e_\gamma(\mathbf{Q}'',J'';l')e^{i\mathbf{Q}\cdot\mathbf{L}'}] .\end{aligned} \tag{18}$$

The prime on the sums denotes that the terms with $(L,l)=(L',l')$ are to be omitted. We can perform the sums over L,L' by taking into account the property of $\phi^{(i)}_{\alpha\beta\gamma}$,

$$\phi^{(i)}_{\alpha\beta\gamma}(L-L';l,l')=-\phi^{(i)}_{\alpha\beta\gamma}(L'-L;l',l) . \tag{19}$$

The sum over L gives a term of the type

$$\sum_{\mathbf{L}}e^{i(\mathbf{Q}+\mathbf{Q}'+\mathbf{Q}'')\cdot\mathbf{L}}=N\Delta(\mathbf{Q}+\mathbf{Q}'+\mathbf{Q}'') , \tag{20}$$

where

$$\Delta(\mathbf{Q})=\begin{cases}1 & \text{if } \mathbf{Q}=\text{two-dimensional reciprocal-lattice vector}\\ 0 & \text{otherwise .}\end{cases}$$

Defining the Fourier transform of $\phi^{(i)}_{\alpha\beta\gamma}(\mathbf{L};l,l')$ as

$$\phi^{(i)}_{\alpha\beta\gamma}(\mathbf{Q};l,l')=\sum_{\mathbf{L}}\phi^{(i)}_{\alpha\beta\gamma}(\mathbf{L};l,l')e^{i\mathbf{Q}\cdot\mathbf{L}} \tag{21}$$

and using the property

$$\phi^{(i)}_{\alpha\beta\gamma}(\mathbf{Q};l,l')=-\phi^{(i)}_{\alpha\beta\gamma}(-\mathbf{Q};l',l)\ , \tag{22}$$

we finally obtain

$$\begin{aligned}V(\mathbf{Q},J;\mathbf{Q}',J';\mathbf{Q}'',J'')=\Delta(\mathbf{Q}+\mathbf{Q}'+\mathbf{Q}'')\frac{2}{12}\left[\frac{\hbar}{M}\right]^{3/2}\frac{1}{\sqrt{N}}[\omega(\mathbf{Q},J)\omega(\mathbf{Q}',J')\omega(\mathbf{Q}'',J'')]^{-1/2}\\ \times\sum_i\sum_j\sum_l\sum_{l'}\sum_{\alpha,\beta,\gamma}\{\phi^{(i)}_{\alpha\beta\gamma}(\mathbf{Q}';l,l')[e_\alpha(\mathbf{Q},J;l')e_\beta(\mathbf{Q}'J';l)e_\gamma(\mathbf{Q}'',J'';l')]\\ +\phi^{(i)}_{\alpha\beta\gamma}(\mathbf{Q}'';l,l')[e_\alpha(\mathbf{Q},J;l')e_\beta(\mathbf{Q}'J';l')e_\gamma(\mathbf{Q}'',J'';l)]\\ +\phi^{(i)}_{\alpha\beta\gamma}(\mathbf{Q};l,l')[e_\alpha(\mathbf{Q},J;l)e_\beta(\mathbf{Q}',J';l')e_\gamma(\mathbf{Q}'',J'',l')]\}\ .\end{aligned} \tag{23}$$

The physical interpretation of the various terms is rather transparent. The first term in the square bracket describes a scattering process in which the phonon $\mathbf{Q},J$ lying on the l'th plane interacts with the phonon $\mathbf{Q}'',J''$ on the same plane, giving rise to a phonon with momentum $\mathbf{Q}',J'$ in the plane l. $V(\mathbf{Q}')$ is the matrix element of the transition. A similar interpretation can be given to the other terms.

In the calculation of anharmonic properties it is necessary to evaluate sums over momenta $\mathbf{Q}'$ and $\mathbf{Q}''$ of the quantity $|V|^2$ multiplied by various functions of momentum and energy. These calculations are rather complex, as is evident from Eq. (23), and generally are simplified with the Peierls approximation,[17] which consists of approximating V as

$$V\sim[\omega(\mathbf{Q},J)\omega(\mathbf{Q}',J')\omega(\mathbf{Q}'',J'')]^{1/2}\ . \tag{24}$$

This is a drastic approximation of Eq. (21) and unfortunately does not give an accurate picture of the dependence of V on the momenta $\mathbf{Q}$ and $\mathbf{Q}'$.

To illustrate this point, we will consider the contribution of the Rayleigh mode to V around the $\bar{\Gamma}$ point. To estimate the polarization vectors, we consider the Rayleigh wave for a continuous medium. In this case[18] the polarization vectors are normal to the surface plane and are given by

$$e_z(\mathbf{Q},J;l)\propto\sqrt{Q}\ , \tag{25}$$

while the frequency is given by

$$\omega(\mathbf{Q},J)=\omega_{\max}\sin\left[\frac{\pi}{2}\frac{Q}{Q_{\max}}\right], \tag{26}$$

where $\omega_{\max}$ is the phonon energy at the zone boundary $Q_{\max}$.

To further simplify the calculations, we take for ω a Debye model so that

$$\omega(\mathbf{Q},J)\propto Q\ , \tag{27}$$

for Q smaller than a suitable Debye momentum. We consider the Al(111) surface and $\mathbf{Q}$ along the $\bar{\Sigma}(11\bar{2})$ direction. For the sake of simplicity we consider nearest-neighbor interactions and the Rayleigh wave entirely localized on the surface. In this way we can put $l=l'=1$ and $J=J'=J''=1$. The Rayleigh wave is also assumed to have a polarization normal to the surface so that we can take $\alpha=\beta=\gamma=z$.

With a simple calculation we get for V a sum of terms of the type

$$\begin{aligned}V(\mathbf{Q},\mathbf{Q}',\mathbf{Q}'')\propto\Delta(\mathbf{Q}+\mathbf{Q}'+\mathbf{Q}'')[\sin(\pi a_L\mathbf{Q})+\sin(\pi a_{L'}\mathbf{Q}')\\ +\sin(\pi a_{L''}\mathbf{Q}'')]\ ,\end{aligned} \tag{28}$$

where $a_L=\hat{Q}\cdot\mathbf{L}$, $a_{L'}=\hat{Q}'\cdot\mathbf{L}$, and $a_{L''}=\hat{Q}''\cdot\mathbf{L}$. For $\mathbf{Q}=0$, Eq. (28) behaves as

$$V(Q,\mathbf{Q}',\mathbf{Q}'')\propto\sin(\pi a_{L'}\mathbf{Q}')\ , \tag{29}$$

while in the Peierls approximation this V coefficient would be zero. This demonstrates the necessity of using the full expression for the V coefficient.

IV. NUMERICAL CALCULATION OF THE PHONON LINEWIDTH

In the present calculations we consider second-order cubic anharmonic central interactions extending up to third neighbors. The imaginary part of the proper self-energy, which determines the linewidth, is given by[3,19]

$$\Gamma(\mathbf{Q},J;\omega)=\frac{18\pi}{\hbar^2}\sum_{\mathbf{G}}\sum_{\mathbf{Q}_1\in\mathrm{SBZ}}\sum_{J_1,J_2}|V(-\mathbf{Q},J;\mathbf{Q}_1,J_1;\mathbf{Q}-\mathbf{Q}_1+\mathbf{G},J_2)|^2$$
$$\times\{(n_1+n_2+1)[\delta(\omega-\omega_1-\omega_2)-\delta(\omega+\omega_1+\omega_2)]$$
$$+(n_1-n_2)[\delta(\omega+\omega_1-\omega_2)-\delta(\omega-\omega_1+\omega_2)]\}\ , \tag{30}$$

where $(\mathbf{Q},J)$ labels the harmonic mode of momentum $\hbar\mathbf{Q}$ corresponding to branch J, $\omega=\omega(\mathbf{Q},J)$, $\omega_i=\omega(\mathbf{Q}_i,J_i)$ $(i=1,2)$, $n_i=n(\omega_i)$ is the occupation number of phonon i, and, for conservation of momentum, $\mathbf{Q}_2=\mathbf{Q}-\mathbf{Q}_1+\mathbf{G}$. If $\mathbf{G}=\mathbf{0}$ and $\mathbf{Q}_2$ lies inside the first SBZ, the process is called normal; otherwise, if a reciprocal-lattice vector is required to return $\mathbf{Q}_2$ to the first SBZ, the process is classified as umklapp. In performing the summations in Eq. (30), we found that the best convergence was obtained by representing the δ function by

$$\delta(\omega)=\frac{1}{\varepsilon\sqrt{\pi}}e^{-\omega^2/\varepsilon^2}\ , \tag{31}$$

where $\varepsilon^2=(\Delta\omega)^2/2\ln 2$ and $\Delta\omega$ is the width of the Gaussian at half maximum. In actual practice, ε must have a finite value that is sufficiently large to give a reasonable number of $\mathbf{Q}$ points a nontrivial weight and yet sufficiently small that the function is sharply peaked. The fulfillment of these conditions also depends on the number of planes in the slab, since increasing the number of planes produces more closely spaced phonon eigenvalues. For a slab of 15–21 planes the above conditions are satisfied with $\Delta\omega=1$ meV, and the evaluated linewidths are sensibly independent of ε over a range of values around 1 meV.

The calculations were performed with a slab of 15 layers, and convergence was checked by performing calculations at some selected points of the SBZ, with a slab of 21 layers. The slab with 15 layers already ensures that interference effects of the modes localized on opposite surfaces are negligible for $Q\geq 0.2$ Å^{-1}. This has been verified by comparing the surface-phonon frequencies obtained with $N_Z=15$ with those obtained with $N_Z=45$.

The $\mathbf{Q}_1$ sum over the SBZ in Eq. (30) requires particular care. By taking an arbitrary mesh in the SBZ, the presence of umklapp processes requires that the sum has to be performed over the whole SBZ. For the (111) surface that we are considering, the umklapp processes are associated with the first two shells of reciprocal-lattice vectors $\mathbf{G}_1$ and $\mathbf{G}_2$. Only a $\mathbf{G}_1$ or a $\mathbf{G}_2$ can remap an arbitrary $\mathbf{Q}_2$ into the first SBZ. The number of terms involved in the multiple sums in Eq. (30) is of the order of N_z^2 values times the number of $\mathbf{Q}$ values inside the SBZ. The number of terms is approximately equal to 10 000 times the number of $\mathbf{Q}_1$ values. To reduce drastically the number of terms in the sums, we have chosen an appropriate mesh of $\mathbf{Q}_1$ values in such a way that $\mathbf{Q}_2\mp\mathbf{G}$ is also a point of the chosen mesh. This choice also reduces drastically the number of diagonalizations of the dynamical matrix. The mesh that fulfills the above requirements is drawn in Fig. 1. The vectors $\mathbf{G}_1$ and $\mathbf{G}_2$ can be written as

$$\mathbf{G}_i=n_i\boldsymbol{\delta}_1+m_i\boldsymbol{\delta}_2\ , \tag{32}$$

where $\boldsymbol{\delta}_1$ and $\boldsymbol{\delta}_2$ are the unit vectors defining the mesh and n_i and m_i are integers. In this way a given $\mathbf{Q}_2$ can be remapped into a point of the mesh inside the irreducible part of the SBZ by subtracting a reciprocal-lattice vector $\mathbf{G}_i$ and eventually by using the symmetry operations of the surface point group (D_{3h}).

When a vector $\mathbf{Q}_2$ is remapped inside the irreducible part of the SBZ, the same symmetry operations should also be applied to the corresponding phonon eigenvectors. With this procedure a mesh point inside the irreducible part is representative of 12 points in the whole SBZ. The number of terms in EQ. (30) is practically reduced by about a factor of 12, which makes the evaluation of Eq. (30) more affordable in terms of computer time. This procedure imposes a limitation on the values of Q for which we can evaluate the linewidth. We can evaluate Γ only at points belonging to the mesh. For example, we show in Fig. 1 the mesh of $\mathbf{Q}=n_1\boldsymbol{\delta}_1+n_2\boldsymbol{\delta}_2$, with $n_1=0,1,2$ and $n_2=0,1,2,3$. Here, $\boldsymbol{\delta}_1$ and $\boldsymbol{\delta}_2$ are the basis vectors depicted in Fig. 1.

We now present our results for $2\Gamma_{\mathrm{RW}}(Q)$, the linewidth of the Rayleigh mode. We first consider the convergence

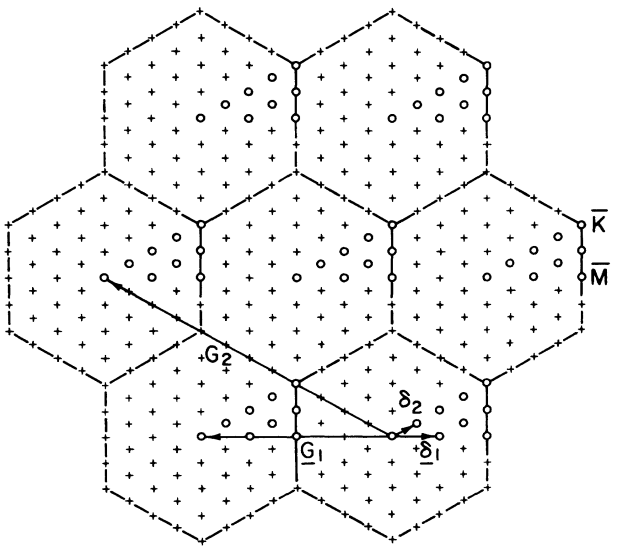

FIG. 1. The hexagonal SBZ of the (111) surface of Al. The $\boldsymbol{\delta}_1$ and $\boldsymbol{\delta}_2$ are the basic vectors that define the mesh used in the calculations. The open dots are in the irreducible part of the SBZ. The crosses are the points in the entire SBZ. The vectors $\{\mathbf{G}_1\}$ and $\{\mathbf{G}_2\}$ are the only reciprocal vectors that remap any $\mathbf{Q}$ point of the extended zone into the SBZ.

of $\Gamma_{RW}(Q)$ as a function of the number of planes N_Z. At the $\bar{M}$ point of the SBZ we consider 21 $\mathbf{Q}_1$ points in the entire first SBZ. The evaluated linewidth is $2\Gamma_{RW}(\bar{M})=0.612$ meV for $N_Z=15$. By varying the value of N_Z, we estimate the probable error to be 0.05 meV. The convergence of $2\Gamma_{RW}(\bar{M})$ as function of the number of $\mathbf{Q}_1$ points is presented in Table II. In the same Table is also given the number of $\mathbf{Q}_1$ values in the entire SBZ as well as in the irreducible part. As one can see from Table II, the convergence is very rapid: It is reached with 16–21 points in the irreducible zone. In order to also have good convergence for the $\mathbf{Q}_1$ inside the SBZ, we performed the calculations with 21 values of $\mathbf{Q}_1$. The results for $\Gamma_{RW}(\mathbf{Q})$ along the $\bar{\Sigma}$ direction are presented in Fig. 2 with the estimated error bars. In the same figure is also drawn the straight line that best fits the calculated results. One sees that the straight line does not pass through the origin. This indicates that $2\Gamma_{RW}(Q)$, in the limit $Q\rightarrow 0$, goes to zero more rapidly than Q.

This result is consistent with the more general result, obtained in the framework of the theory of elasticity by Mayer and Bortolani.[20] According to these authors

$$2\Gamma_{RW}(Q) \underset{\lim Q\rightarrow 0}{\propto} Q^{11/3} .$$

In Table II the normal and umklapp contributions to the linewidth are also given. One sees that the umklapp contributions have the same importance as the normal ones. This important result was also found in the evaluation of the linewidth for bulk phonons.

We wish to point out that the value of $2\Gamma_{RW}$ at the $\bar{M}$ point, where the mode is purely transverse, is much larger than the maximum value of 2Γ attained by transverse modes in the bulk.[12] This is proof of the importance of anharmonicity in the surface region and is consistent with the notion that in the surface region the atoms are more weakly bound than in the bulk region.

In Fig. 2 we have included the experimental value[11] of $2\Gamma_{RW}$ at the $Q=0.8Q_{\bar{M}}$ point. As one can see, the agreement between the calculated and experimental values is good, particularly when one notes that the complicated deconvolution procedure required to extract the value of 2Γ from the experimental data introduces additional uncertainty into the experimental values. Furthermore, the deconvolution corrections increase with decreasing wave vector, so we have only presented the experimental result for the maximum measured Q. We have also studied the temperature dependence of the linewidth. In Fig. 3 we present the behavior of $2\Gamma_{RW}$ versus T at the $\bar{M}$ point. One sees a linear behavior at high temperatures. This is due to the fact that $n(\omega)$ can be approximated as $k_BT/\hbar\omega$. At $T=0$ the linewidth is associated with the zero-point motion for which $n(\omega)=0$. At very low T the behavior is exponential because

TABLE II. N_{irr} is the number of Q points in an irreducible part of the SBZ. N_{BZ} is the number of points in the whole SBZ. $2\Gamma^N(\bar{M})$, contribution to the linewidth due to normal processes. $2\Gamma^U(\bar{M})$, contribution due to umklapp processes.

$$2\Gamma(\bar{M})=2\Gamma^N(\bar{M})+2\Gamma^U(\bar{M}) ,$$

total linewidth evaluated at the $\bar{M}$ point. Calculation performed at $T=300$ K.

N_{irr}	N_{BZ}	$2\Gamma^N(\bar{M})$	$2\Gamma^U(\bar{M})$	$2\Gamma(\bar{M})$
4	21	0.378	0.234	0.612
9	65	0.391	0.338	0.729
16	133	0.466	0.433	0.899
25	225	0.449	0.429	0.878

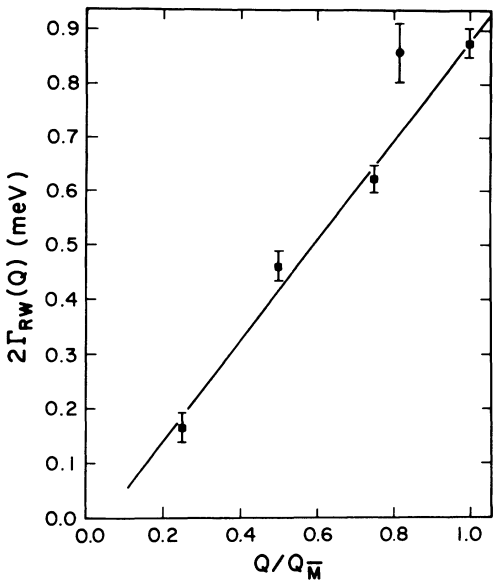

FIG. 2. Linewidth for the Rayleigh mode of Al(111) along the $\bar{\Sigma}$ direction at $T=300$ K. The solid squares are the evaluated linewidth and the straight line is the best fit of the evaluated points. The solid dot represents the experimental point. The estimated errors are also indicated.

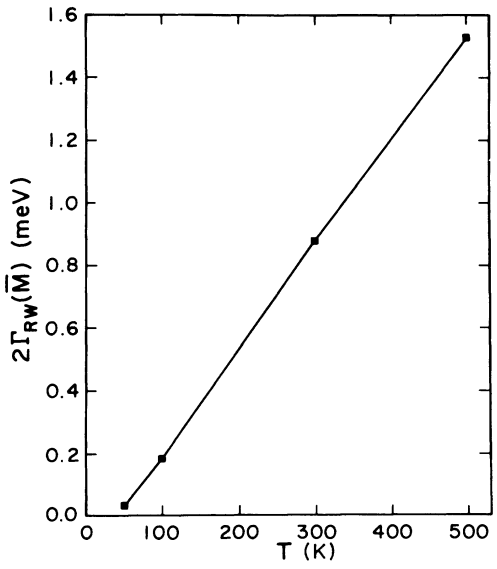

FIG. 3. Linewidth for the Rayleigh mode at the $\bar{M}$ point of Al(111) evaluated as a function of the temperature. Solid squares as in Fig. 2.

$$n(\omega) \propto \exp(-\hbar\omega/k_B T) .$$

The temperature dependence of the linewidth has not yet been measured experimentally at the $\bar{M}$ point.

V. CONCLUSIONS

We have carried out a theoretical analysis of the linewidth of the Rayleigh surface mode of the (111) surface of aluminum for $\mathbf{Q}$ in the $\bar{\Sigma}$ direction. A novel feature of this study is that we have used, for the harmonic part of the interaction, a phenomenological model that contains central interactions extending up to tenth neighbors and angular interactions up to second neighbors. This model reproduces with great accuracy the phonon eigenvalues and eigenvectors derived from *ab initio* pseudopotential calculations both for bulk phonons and for surface phonons. For the anharmonic part, as in our previous[12] study of the linewidth of bulk phonons, we have used central interactions extending up to third neighbors. This ensures convergences of the third-order nearest-neighbor force constant, which is the leading term of the anharmonic interactions. The calculated values of $\Gamma_{RW}(\mathbf{Q})$ exhibit a linear dependence of Γ_{RW} versus Q except at $Q \rightarrow 0$.

We have also seen that $2\Gamma_{RW}(\bar{M})$ is much larger than the maximum linewidth of bulk phonons, which proves the importance of anharmonic effects in the surface region. The result for $2\Gamma_{RW}$ at $Q/Q_{\bar{M}}=0.8$ is in good agreement with the experimental data. Furthermore, we have analyzed the dependence of Γ on the temperature. At high temperature we obtain a linear behavior, as expected from the limiting form of the Bose factor. At very low temperatures the zero-point motion gives rise to a nonzero value of $2\Gamma_{RW}$, which in principle can be measured.

ACKNOWLEDGMENTS

Partial financial support from the Consiglio Nazionale delle Ricerche (Contract No. 89.00011.69), NATO Grant No. 330673/88, and the Ministero dell'Università e della Ricerca Scientifica e Tecnologica is acknowledged by some of us (V.B., G.S., and A.F.). Part of the calculations were performed at the CICAIA of the University of Modena. The work of A.A.M. and R.F.W. was supported in part by NSF Grant Nos. DMR-8918184 and INT-8814951. We would like to thank J. P. Toennies and A. Lock for making available to us their experimental data prior to publication.

*Permanent address: Dipartimento di Fisica, Università degli Studi di Modena, Via Campi 213/A, 41100 Modena, Italy.

[1]L. van Hove, Phys. Rev. **95**, 249 (1954).
[2]R. J. Glauber, Phys. Rev. **98**, 1092 (1955).
[3]A. A. Maradudin and A. E. Fein, Phys. Rev. **128**, 2589 (1962).
[4]R. Stedman and G. Nilsson, Phys. Rev. **145**, 492 (1966).
[5]A. Larose and B. N. Brockhouse, Can. J. Phys. **54**, 1990 (1976).
[6]A. Trayanov and E. Tosatti, Phys. Rev. Lett. **59**, 2207 (1987).
[7]J. W. Frenken and J. F. van der Veen, Phys. Rev. Lett. **54**, 134 (1985).
[8]J. W. Frenken, P. M. J. Maree, and J. F. van der Veen, Phys. Rev. B **34**, 7506 (1986).
[9]C. S. Jayanthi, E. Tosatti, and L. Pietronero, Phys. Rev. B **31**, 3456 (1985).
[10]G. Armand and P. Zeppenfeld, Phys. Rev. B **40**, 5936 (1989).
[11]A. Lock (private communication); J. P. Toennies *et al.* (unpublished).
[12]M. Zoli, G. Santoro, V. Bortolani, A. A. Maradudin, and R. F. Wallis, Phys. Rev. B **41**, 7507 (1990).
[13]R. F. Wallis, A. A. Maradudin, V. Bortolani, A. G. Eguiluz, A. Franchini, and G. Santoro (unpublished).
[14]A. Franchini, V. Bortolani, V. Celli, A. G. Eguiluz, J. A. Gaspar, M. Gester, A. Lock, and J. P. Toennies (unpublished).
[15]*Functional Relationships in Science and Technology,* edited by K. H. Hellwege, Landolt-Börnstein, New Series, Group III, Vol. 2, Pt. 3 (Springer, Berlin, 1979).
[16]J. A. Gaspar, A. G. Eguiluz, M. Gester, A Lock, and J. P. Toennies, Phys. Rev. Lett. **66**, 337 (1991).
[17]R. E. Peierls, *Quantum Theory of Solids* (Oxford University Press, Oxford, England, 1955), p. 38.
[18]L. D. Landau and E. M. Lifshitz, *Theory of Elasticity* (Pergamon, Oxford, England, 1970), Sec. 24; see also D. Eichenauer, U. Harten, J. P. Toennies, and V. Celli, J. Chem. Phys. **86**, 3693 (1987).
[19]E. Haro, M. Balkanski, R. F. Wallis, and K. H. Wanser, Phys. Rev. B **34**, 5358 (1986).
[20]A. P. Mayer and V. Bortolani, Phys. Rev. B **39**, 9912 (1989).